Hydrothermal alteration and main structures mapping using TM images in La Primavera geothermal field (Mexico)

Fernández de la Vega-Márquez, T.[1], R. M. Prol-Ledesma[2] and G. Orozco[3]

[1] *Facultad de Filosofía, UNAM, México*

[2] *Instituto de Geofísica, UNAM, México*

[3] *Schlumberger, Melbourne, Australia*

RESUMEN

Imágenes Landsat TM del campo geotérmico de La Primavera se utilizaron para identificar estructuras principales, y localizar áreas que presentan alteración hidrotermal. Los métodos utilizados en el procesamiento de las imágenes incluyen análisis estadístico univariado y multivariado, así como realce espectral y espacial. La vegetación en el área no se compone de plantas con hojas grandes; sin embargo, sí se presenta interferencia entre el espectro de la vegetación y él de la alteración hidrotermal. Para superar esta interferencia, se utilizaron la técnica de Crosta y el método de Loughlin (Crosta and Moore 1989; Loughlin 1991). Como resultado de este procesado, se logró detectar la presencia de minerales que contienen óxidos de hierro e hidroxilos. Las imágenes resultantes fueron desplegadas en tonos de gris y en composiciones de falso color para resaltar las estructuras principales y las rocas alteradas, respectivamente. Las zonas de alteración identificadas presentan una correlación con los flujos de descarga del yacimiento geotérmico, así como con las estructuras principales que controlan la permeabilidad del yacimiento y de la capa sello. Por lo tanto, la localización en la superficie de las rocas alteradas será de gran utilidad en la identificación de la presencia de descargas de fluidos del yacimiento geotérmico.

PALABRAS CLAVE: Geotermia, alteración, imágenes TM, percepción remota, México.

ABSTRACT

Landsat TM images of the La Primavera geothermal field area were used to identify the main structures within the field, and to locate areas that show hydrothermal alteration. The methods used in the processing of the images include univariate and multivariate statistical analysis, spectral and spatial enhancement. Vegetation in the area is not composed by wide leaf plants; however, there is interference between the spectra of vegetation and hydrothermal alteration. In order to overcome this interference, the Crosta technique and the Loughlin method were used (Crosta and Moore 1989; Loughlin 1991). As a result, iron oxides and hydroxyl minerals were detected in the area. The resulting images were displayed in gray tones and false color composites to enhance main structures and the altered rocks respectively.

The identified alteration zones were correlated with the discharged flows from the geothermal reservoir, and with the main structures that control the permeability of the reservoir and the cap rock; therefore, locating hydrothermally altered rocks in the surface will help to determine the presence of upflows from the geothermal reservoir.

KEY WORDS: Geothermal, alteration, TM images, remote sensing, Mexico.

INTRODUCTION

Geothermal energy exploration with satellite images is useful in the early stages of exploration. Thematic mapping multispectral images from Landsat satellites cover the visible and infrared spectrum of hydrothermal alterations (Hunt 1977, 1979; Hunt and Ashley, 1979). Identification of alterations in a geothermal area may be used to locate faults that generate secondary permeability. The use of satellite images in geothermal exploration has been reported in a few cases (Mongillo *et al.,* 1995; Deroin *et al.,* 1996). However, in mining exploration, satellite images have been widely used to identify hydrothermally altered areas and to identify faults and areas of mineralization (Goetz and Rowan, 1983;

Kauffmann 1988; Crosta and Moore 1989; Loughlin 1991; Wester, 1992; Van der Meer *et al.,* 1995).

La Primavera geothermal field (Figure 1) is located in the western Mexican Volcanic Belt (MVB), 15 km NW of Guadalajara (103º28'-103º43' W and 20°32'-20° 43'N). The field is located in the intersection of the Colima, Chapala and Tepic grabens (Luhr *et al.,* 1995). The Tepic fault system is the most important in the region (Kruger, 1988), and it generates the secondary permeability that characterizes the reservoir.

The geothermal field is located in a rhyolitic volcanic complex (Mahood, 1980). The oldest eruptive activity re-
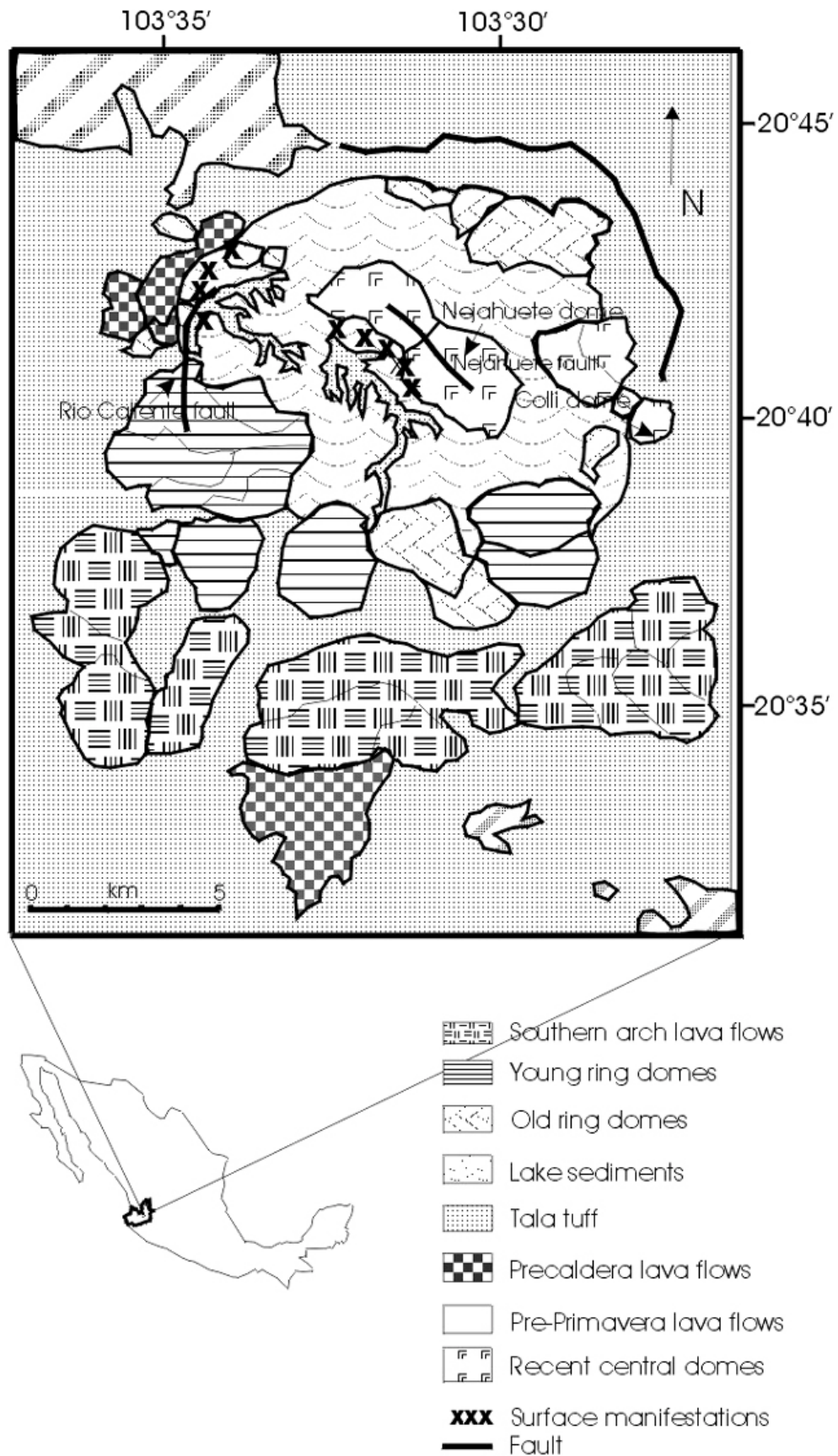
Fig. 1. General location and geology of the caldera La Primavera (after Mahood, 1980).

ported is 120 000 years, followed by a strong explosive event about 95 000 years ago that produced the Tala tuff with a volume of approximately 25 km³. This eruption caused the collapse of the magmatic chamber and the formation of an 11-km diameter caldera surrounded by rhyolitic domes. This caldera contained a lake where sedimentation took place. Volcanic activity resumed with the eruption of rhyolitic domes in the southern part of the caldera. The latest activity formed the central Nejahuete and Colli domes, about 20 000 years ago (Figure 1). The caldera collapse generated local faults striking NW-SE and NE-SW.

After the dome eruption, a hydrothermal system developed with hot springs and fumaroles (Mahood *et al.,* 1983; Gutiérrez-Negrín, 1991). Surface manifestations are located along faults that strike NW-SE, NE-SW and N-S.

SPECTRAL RESPONSE OF HYDROTHERMAL ALTERATION MINERALS

Thematic Mapper bands are too wide to allow the identification of single minerals; however, they serve to identify groups of minerals for exploration purposes in the near and

middle infrared, belonging to the hydroxyl and sulfate groups. Iron oxide is frequently observed in the outcrops of hydrothermally altered rocks as a result of weathering; its identification is a useful key to define areas that contain weathered hydrothermally altered rocks.

These minerals have spectral features in the visible and infrared parts (0.4 - 2.5 μm) (Figure 2). The main problem in the identification of the minerals is the interference from vegetation that also has a strong reflectance in the infrared. When iron oxides are present, the rock color is red, brown, orange or yellow. The presence of clay minerals usually yield pale yellow, violet, green or beige. The jarosite reflectance curve shows well defined absorption features at 0.43 and 0.92 μm; hematite has a reflectance minimum at 0.85μm, and goethite at about 0.94 μm (Hunt and Ashley, 1979). Absorption anomalies at wavelengths less than 0.9 μm are a good indication of hematite. When the anomalies are at wavelengths above 0.9 μm, jarosite or goethite are more abundant (Hunt and Ashley, 1979).

The middle infrared region of the spectrum, between 1.1 and 2.5 μm, can provide more information about the min-
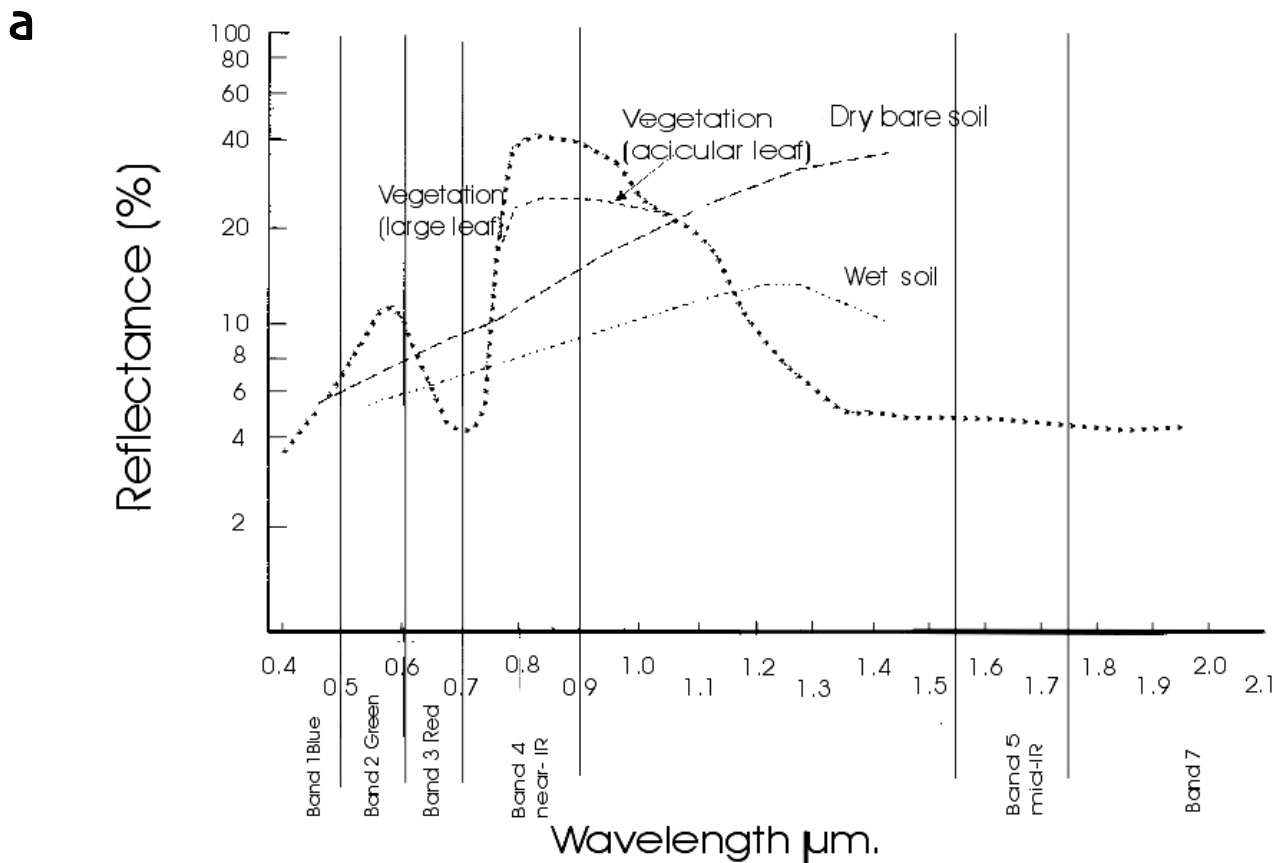
Fig. 2.- Spectra of materials to be identified in the studied image: a) vegetation (large and acicular leaf); b) oxide and c) hydroxyl minerals (after Hunt 1977, 1979; Hunt and Ashley, 1979)

b

TM 1 TM 2 TM 3 TM 4

Jarosite

Hematite

Goethite

100
80
60
40
20
10
8
6
4
2

Reflectance log. (%)

0.4   0.6   0.8   1.0
  0.5   0.7   0.9

Wavelength (μm)
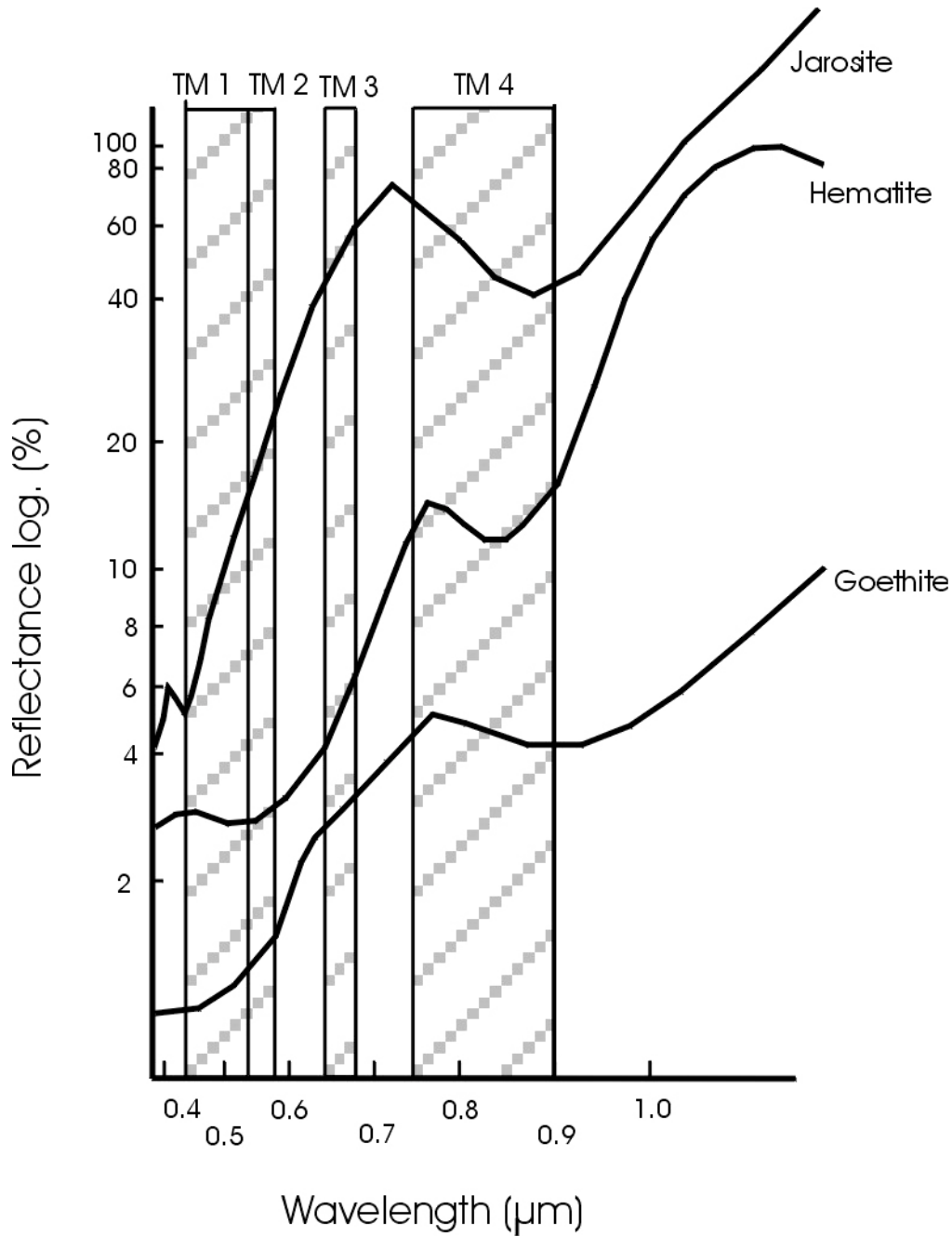
Fig. 2. Continued.

eralogical composition than the spectral features observed in the visible and near infrared regions. The middle infrared contains high reflectance anomalies for most rocks (basalt, gabbro, etc.) and minerals (clays, micas, sulfates, carbonates) at about 1.65 μm and high absorption at approximately 2.2 μm (Goetz and Rowan 1983).

Vegetation shows absorption features from 0.45 to 0.68 μm, and high reflectance in the near infrared, between 1.6

μm and 2.2 μm, due to the chlorophyll absorption. The absorption bands at about 1.4 μm and 1.9 μm are related to the water content.

Iron oxides and vegetation show similar reflectance in TM Band 1 (0.45-0.52 μm) and TM Band 2 (0.52-0.60 μm), therefore these bands are not very useful for separating these materials. On the other hand, TM3 band (0.63-0.69 μm) shows high reflectance for the iron oxides and a strong ab-

C
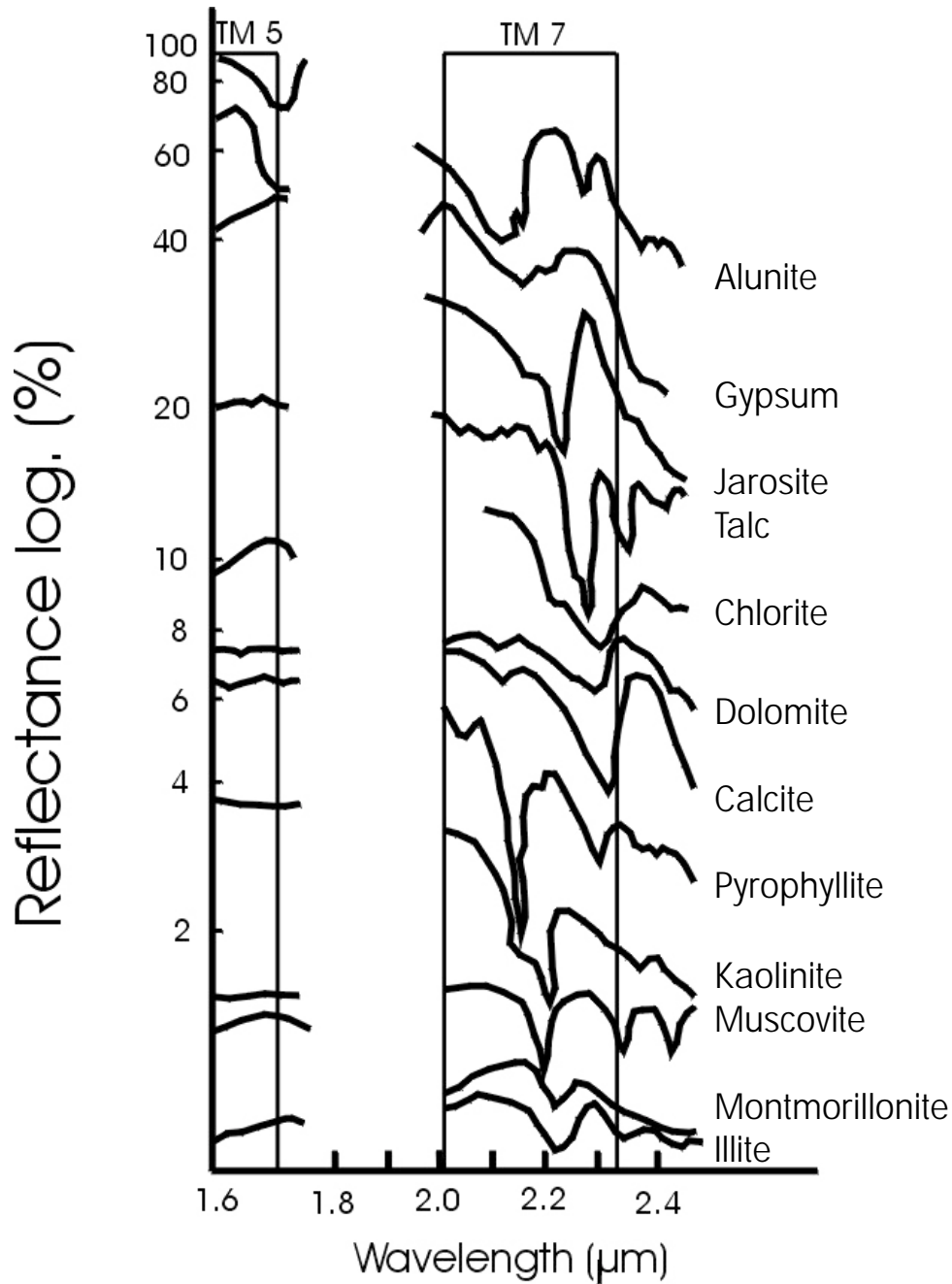
Fig. 2. Continued.

sorption for vegetation. This is useful to differentiate oxides from vegetation (Figure 2 a, b, c). Band TM4 (0.76-0.90 μm) is used for vegetation identification; it contains also an absorption band for iron oxides at 0.90 μm. Both features can be used to separate oxides from vegetation.

TM5 (1.55-1.75 μm) and TM7 (2.08-2.35 μm) bands are very helpful for distinguishing vegetation from hydroxyl and iron oxides.

IMAGE PROCESSING

A section from the Thematic Mapper (TM) Landsat 5 image (path 29- row 46), taken in April 1992, which contains La Primavera geothermal field, was used in this study. The thermal band was not used because of its low resolution (100 m^2 pixel).

Preprocessing of the image included radiometric correction to remove the atmospheric effects. The correction
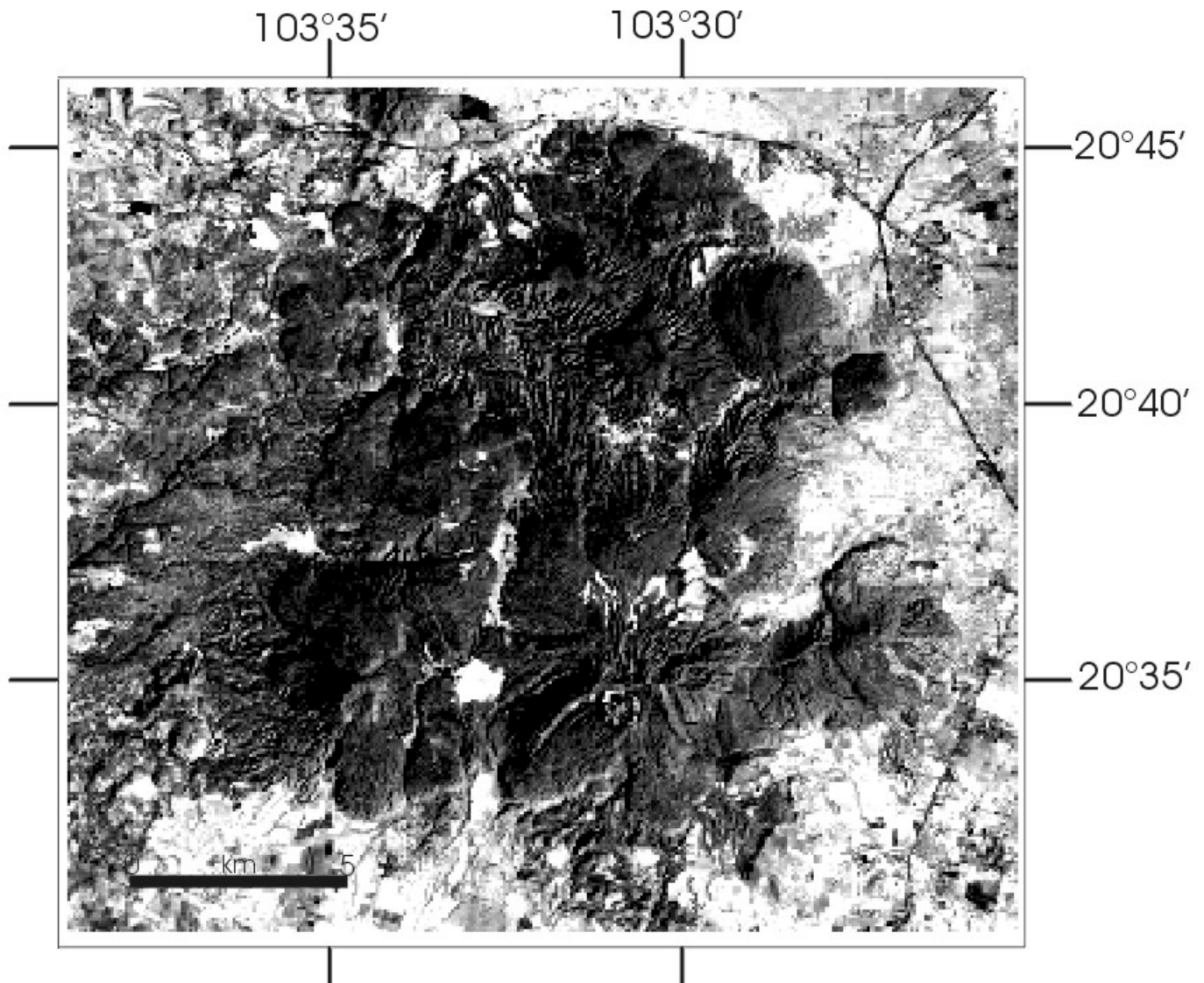
Fig. 3.- Display in 256 tones of grey of La Primavera TM image band 5.

was calculated according to Jensen (1996), by subtracting the minimum values for each band. No other corrections were applied as the image did not show stripping or line drop-outs. Band 5 is shown in Figure 3 after stretching with saturation of 5% of the histogram was performed.

We enhanced the spectral response of hydrothermal alteration minerals to identify surface hydrothermal activity in the study area. The information contained in the bands of the La Primavera image is displayed using color composites, after band ratio and principal component analysis. The identification of altered rocks is performed by comparison of the spectral response of the alteration minerals and the DN of the pixels in the bands of the image. In addition to the identification of the alteration minerals, the vegetation was identified and its response minimized.

False color composites included the bands where the spectral response of the minerals indicates a maximum in their reflectance. This enhancement is achieved by combining bands in the visible and the infrared (Crosta and Moore 1989; Drury,1990).

The false color composite (RGB) of bands TM4, TM3 and TM2 was obtained with the aim of displaying the oxide minerals in green and vegetation in red (Figure 4). Urban areas have a similar reflectance in the three bands used in this composite (Jensen,1996); they are displayed in grey tones.

152
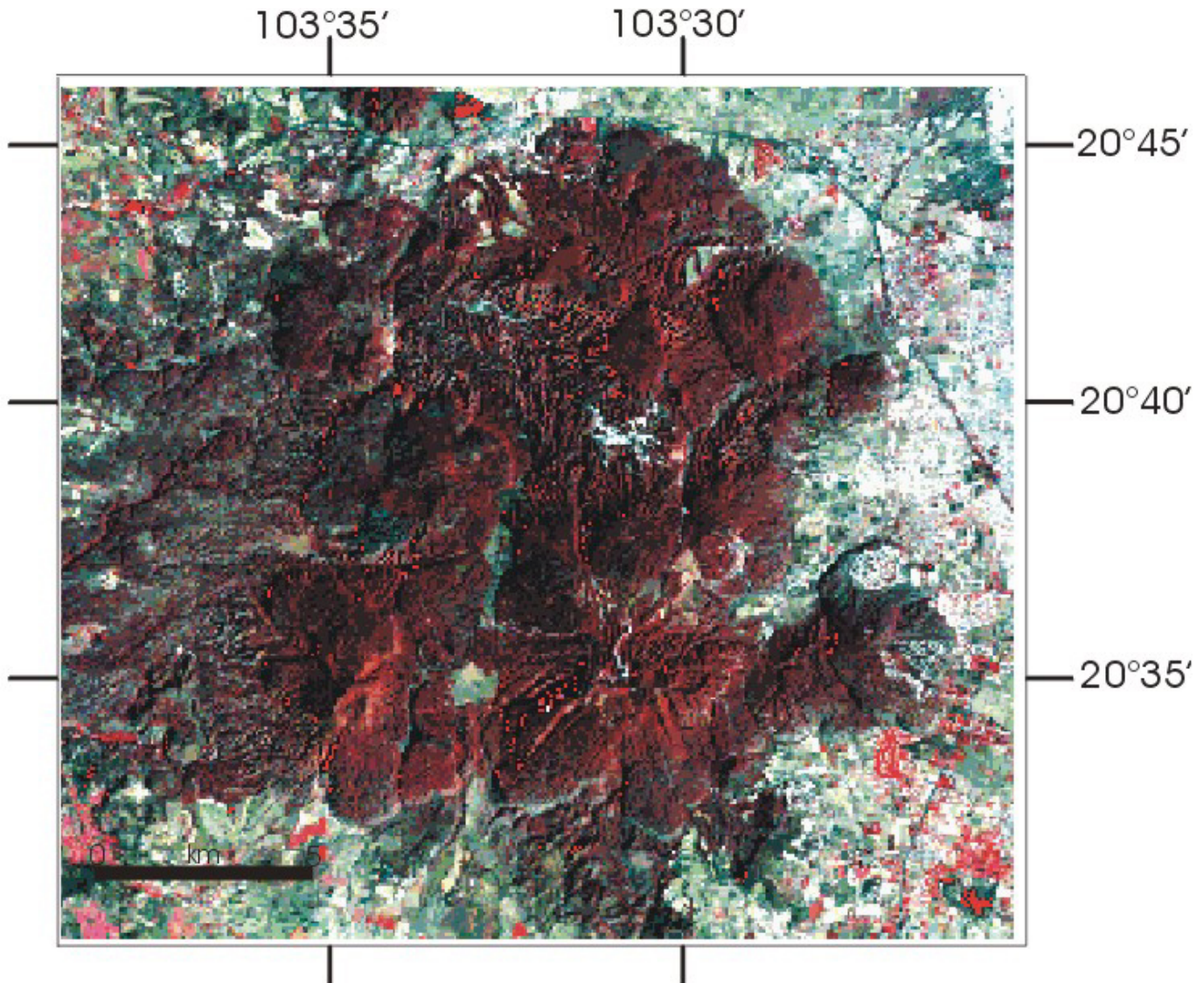
Fig. 4.- RGB color composition using the bands: R-4, G-3, B-2.

Hydrothermally altered areas are better defined in the composite that includes bands TM7, TM4 and TM2, where alteration is shown in red.

Color composite yields a good discrimination of hydrothermal minerals, when their spectra do not overlap with the spectra of the materials present in the image. Otherwise, traditional processing includes calculation of band ratios, as a method for enhancing the response of the minerals and reducing the vegetation response. Band ratios were obtained for bands 4/3, 5/4 and 5/7 for identification of vegetation and hydrothermal alteration.

In order to display simultaneously the results of the three band ratios, a color composite image was generated (Figure 5). According to the spectral characteristics of the minerals and the color composition used (R-5/4, G-4/3, B-5/7), hydrothermally altered rock should appear blue, red and magenta, as shown in Figure 5. In the case of La Primavera geothermal field, the band ratios did not yield good results because of the vegetation cover in the area.

Principal Component Analysis (PCA) of TM images has been shown to be a successful tool to minimize the vegetation effect (Crosta and Moore 1989; Loughlin 1991; Ruíz-Armenta and Prol-Ledesma, 1998).

In order to differentiate the areas containing hydrothermal minerals from those that contained only vegetation, sta-
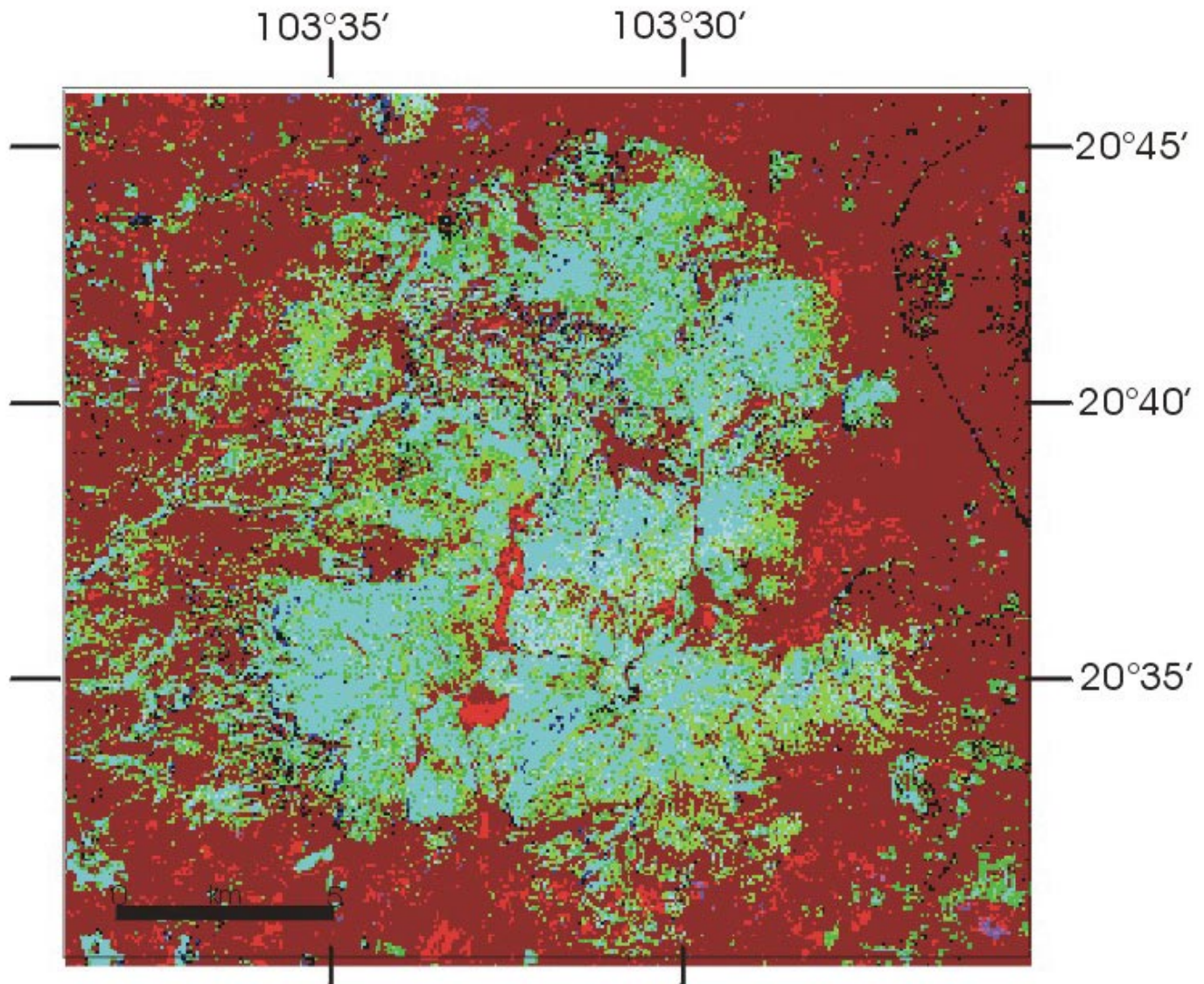
Fig. 5.- RGB color composition using the band ratios: R-5/4, G-4/3, B-5/7.

tistical techniques based on the analysis of principal components were applied to the images (Chavez and Yaw Kwarteng 1989), taking into account the spectral characteristics of the minerals.

The results of PCA of six bands in the La Primavera image are presented in Table 1. The correlation matrix shows that the three bands in the visible are highly correlated; also the middle infrared bands have a high correlation. The first principal component contains 91.98% of the variance.

Component 5 shows oxide areas as dark pixels, and component 4 shows the hydroxyl minerals. The negative of these images would display the altered areas as bright pix-

els. Vegetation spectral response is contained in principal component 2 as bright pixels.

False color composition of the images corresponding to the negative of component 5 (R), component 4 (G) and the sum of both in the blue channel (O, H, O+H) allows the identification of altered rocks (Figure 6).

SPATIAL ENHANCEMENT

The fractures and faults in the rocks are commonly shown like borders or segments of lines that form "lineaments" in aerial photographs and satellite images (Ruiz-Armenta and Prol-Ledesma, 1995. These lineaments can be

Table 1

Results of the Principal Components Analysis of La Primavera image:
variance-covariance matrix, correlation matrix and band load matrix.

VAR/COVAR	primab1	primab2	primab3	primab4	primab5	primab7
primab1	140.19	91.55	142.72	80.89	255.76	185.68
primab2	91.55	61.81	96.26	57.89	174.04	124.83
primab3	142.72	96.26	153.92	88.75	287.16	205.06
primab4	80.89	57.89	88.75	88.90	169.16	109.20
primab5	255.76	174.04	287.16	169.16	666.39	446.90
primab7	185.68	124.83	205.06	109.20	446.90	317.24

COR MATRX	primab1	primab2	primab3	primab4	primab5	primab7
primab1	1.000000	0.983511	0.971591	0.724622	0.836777	0.880499
primab2	0.983511	1.000000	0.986887	0.780947	0.857538	0.891500
primab3	0.971591	0.986887	1.000000	0.758755	0.896625	0.927983
primab4	0.724622	0.780947	0.758755	1.000000	0.695011	0.650259
primab5	0.836777	0.857538	0.896625	0.695011	1.000000	0.971976
primab7	0.880499	0.891500	0.927983	0.650259	0.971976	1.000000

COMPONENT	C 1	C 2	C 3	C 4	C 5	C 6
% var.	91.98	4.76	2.56	0.44	0.21	0.04
eigenval.	1313.92	68.01	36.63	6.35	2.97	0.55
eigvec.1	0.297454	0.496127	-0.366203	-0.187773	-0.655065	-0.258661
eigvec.2	0.202082	0.327144	-0.130823	-0.083683	0.078691	0.906548
eigvec.3	0.327749	0.379665	-0.230329	-0.182935	0.745878	-0.324938
eigvec.4	0.192786	0.485595	0.795463	0.294938	-0.045387	-0.072253
eigvec.5	0.701240	-0.474271	0.281654	-0.444123	-0.079363	0.021371
eigvec.6	0.484108	-0.204826	-0.289203	0.800025	-0.002290	-0.001686

LOADING	C 1	C 2	C 3	C 4	C 5	C 6
primab1	0.910647	0.345564	-0.187180	-0.039965	-0.095373	-0.016271
primab2	0.931741	0.343171	-0.100707	-0.026824	0.017255	0.085886
primab3	0.957599	0.252376	-0.112357	-0.037158	0.103639	-0.019508
primab4	0.741164	0.424735	0.510583	0.078829	-0.008298	-0.005708
primab5	0.984661	-0.151514	0.066030	-0.043355	-0.005300	0.000617
primab7	0.985226	-0.094838	-0.098266	0.113191	-0.000222	-0.000071
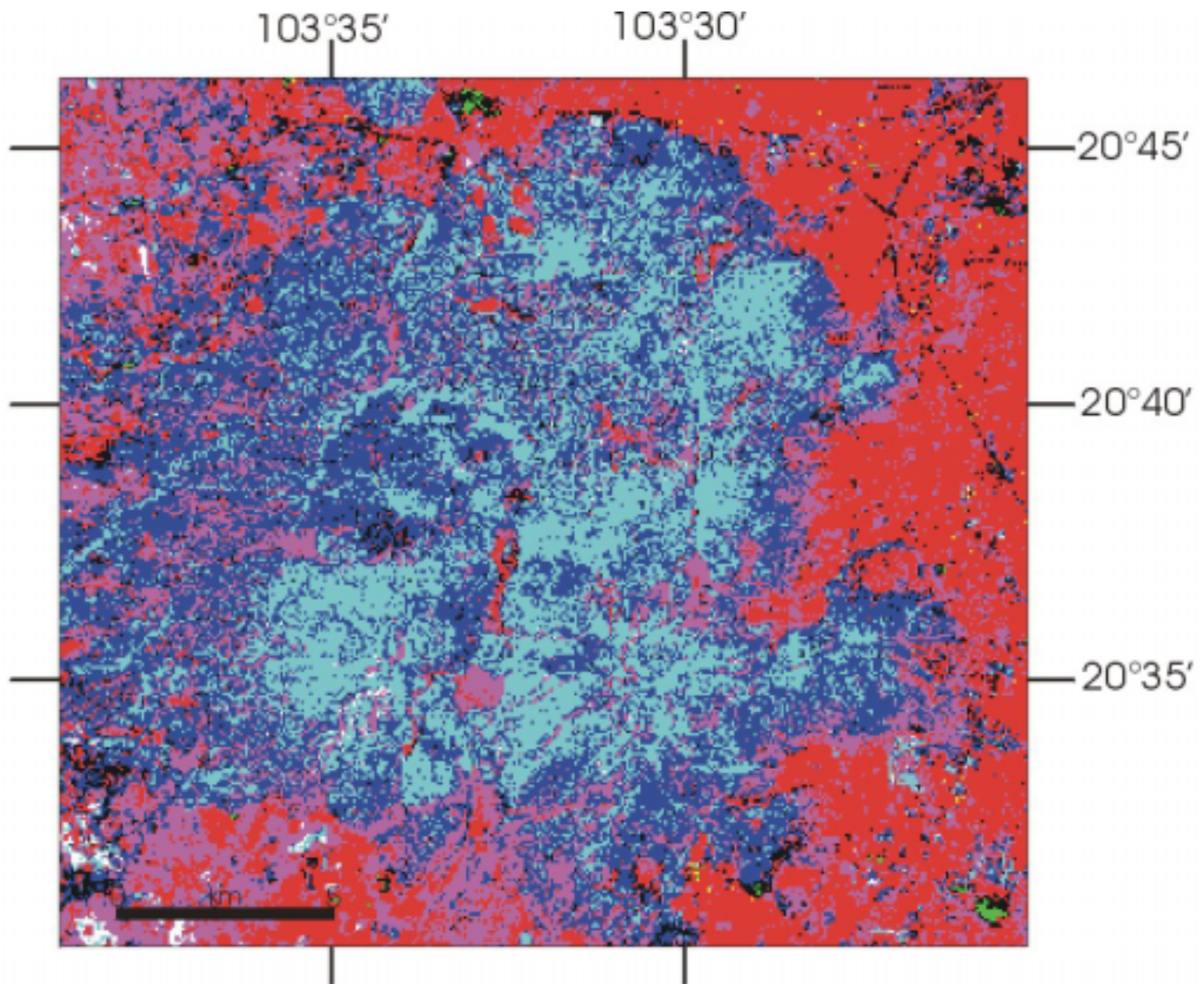
Fig. 6.- Oxide and hydroxyl minerals identified using the principal components analysis of the 6 non-thermal bands of La Primavera image. False color composition using the band ratios: R-3/1, G-5/7, B-O+H.

formed by a variety of elements of the landscape, including topography, tectonics, drainage, vegetation and tones of the soil or rock. Almost all lineaments are discontinuous (Ruiz-Armenta and Prol-Ledesma, 1995).

Spatial enhancement was applied to the La Primavera image, with the purpose of bringing out the predominant fault systems, and to determine their relationship to the hydrothermal activity of the area.

Spatial enhancement was performed on the first principal component PC1, that contains 91.98% of the variance, and therefore it contains information related with the topography and the albedo of the six non thermal bands.

Figure 7 shows the results of the edge Laplacian enhancement filter. The caldera is clearly observed. The faults related to the rhyolitic domes within and in the borders of the caldera are enhanced (see Figure 7).

The method developed by Moore and Waltz (l983) was used with the purpose of extracting the size, location and orientation of lineaments. This method consists of 5 steps:

1) Removing the high frequencies (noise) with a low-pass filter.

2) Generation of directional components with convolution algorithms. In this step the contrast of borders and seg-
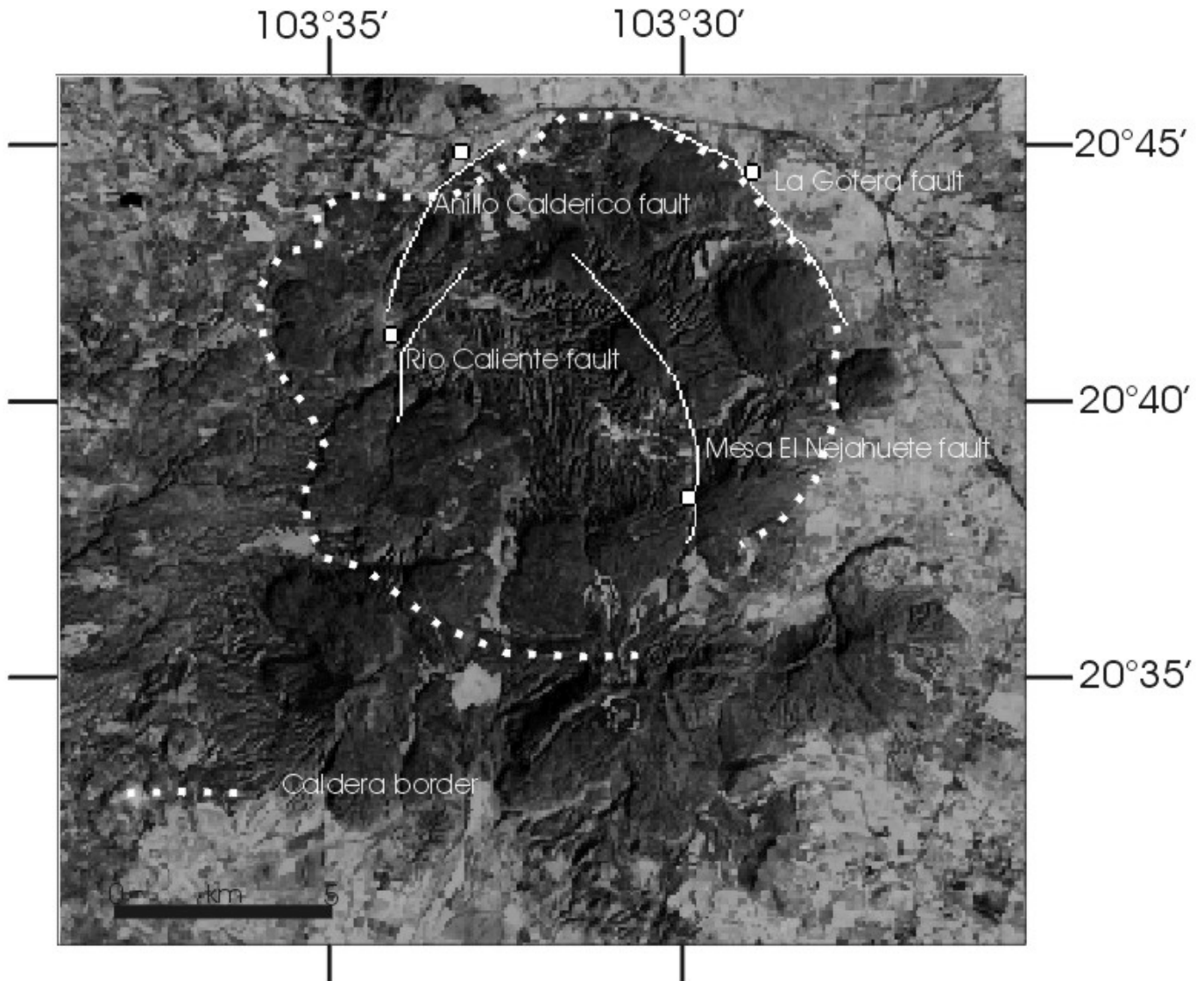
Fig. 7.- Laplacian Edge Enhancement filter applied to the first principal component of the La Primavera image. Lines indicate faults checked in the field.

ments of lines is increased only for those lineaments perpendicular to the applied kernel (Ruiz-Armenta and Prol-Ledesma, 1995).

3) A low-pass filter is applied again to the image after step 2, in order to reduce the creation of artificial lineaments in the filter direction.

4) Extraction of segments of lines and prominent borders. The brightness values of the smoothed image from step (3) are enhanced for visualization by applying a contrast stretch with 2% saturation.

5) The visualization is improved by adding the obtained image to the first principal component.

The kernels used in step (2) are Prewitt filters (Table 2). They were applied in all directions. The fracturing within the field is controlled mainly by the stages of maximum deformation related to the caldera formations that may have reactivated older structures in the reservoir strata related to the three structural systems in the surroundings of the La Primavera geothermal field: E-W (Chapala graben), N-S (Colima graben) and NW-SE (Tepic graben) (Garduño and López, 1986).

The best results were obtained with filters NE-SW and NW-SE, wich are perpendicular and paralell, respectively, to one of the main fault systems. The results are shown in Figures 8 and 9 respectively.

157

Table 2

Prewitt filters.

$$N = \begin{pmatrix} 1 & 1 & 1 \\ 1 & -2 & 1 \\ -1 & -1 & -1 \end{pmatrix} \qquad S = \begin{pmatrix} -1 & -1 & 1 \\ 1 & -2 & 1 \\ 1 & 1 & 1 \end{pmatrix} \qquad E = \begin{pmatrix} -1 & 1 & 1 \\ -1 & -2 & 1 \\ -1 & 1 & 1 \end{pmatrix}$$

$$W = \begin{pmatrix} 1 & 1 & 1 \\ 1 & -2 & -1 \\ 1 & 1 & -1 \end{pmatrix} \qquad NE = \begin{pmatrix} 1 & 1 & 1 \\ -1 & -2 & 1 \\ -1 & -1 & 1 \end{pmatrix} \qquad NW = \begin{pmatrix} 1 & 1 & 1 \\ 1 & 2 & 1 \\ 1 & -1 & -1 \end{pmatrix}$$

$$SE = \begin{pmatrix} -1 & -1 & 1 \\ -1 & -2 & 1 \\ 1 & 1 & 1 \end{pmatrix} \qquad SW = \begin{pmatrix} 1 & -1 & -1 \\ 1 & -2 & -1 \\ 1 & 1 & 1 \end{pmatrix} \qquad Laplacian = \begin{pmatrix} 0 & -1 & 0 \\ -1 & 5 & -1 \\ 0 & -1 & 0 \end{pmatrix}$$
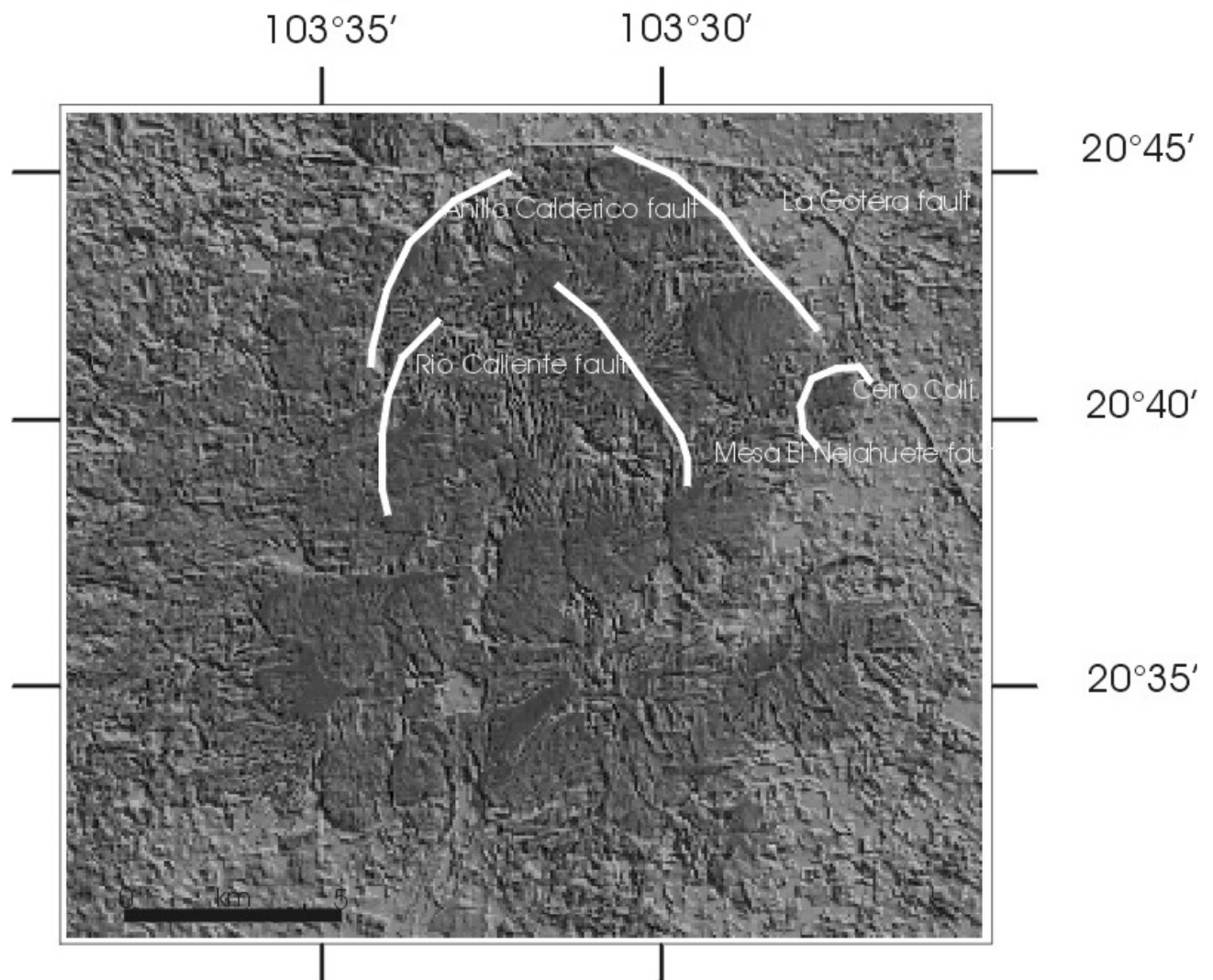
Fig. 8.- NE quadrant of La Primavera image resulting of application of NE-SW directional filter. Lines indicate faults and dots- surface manifestations.
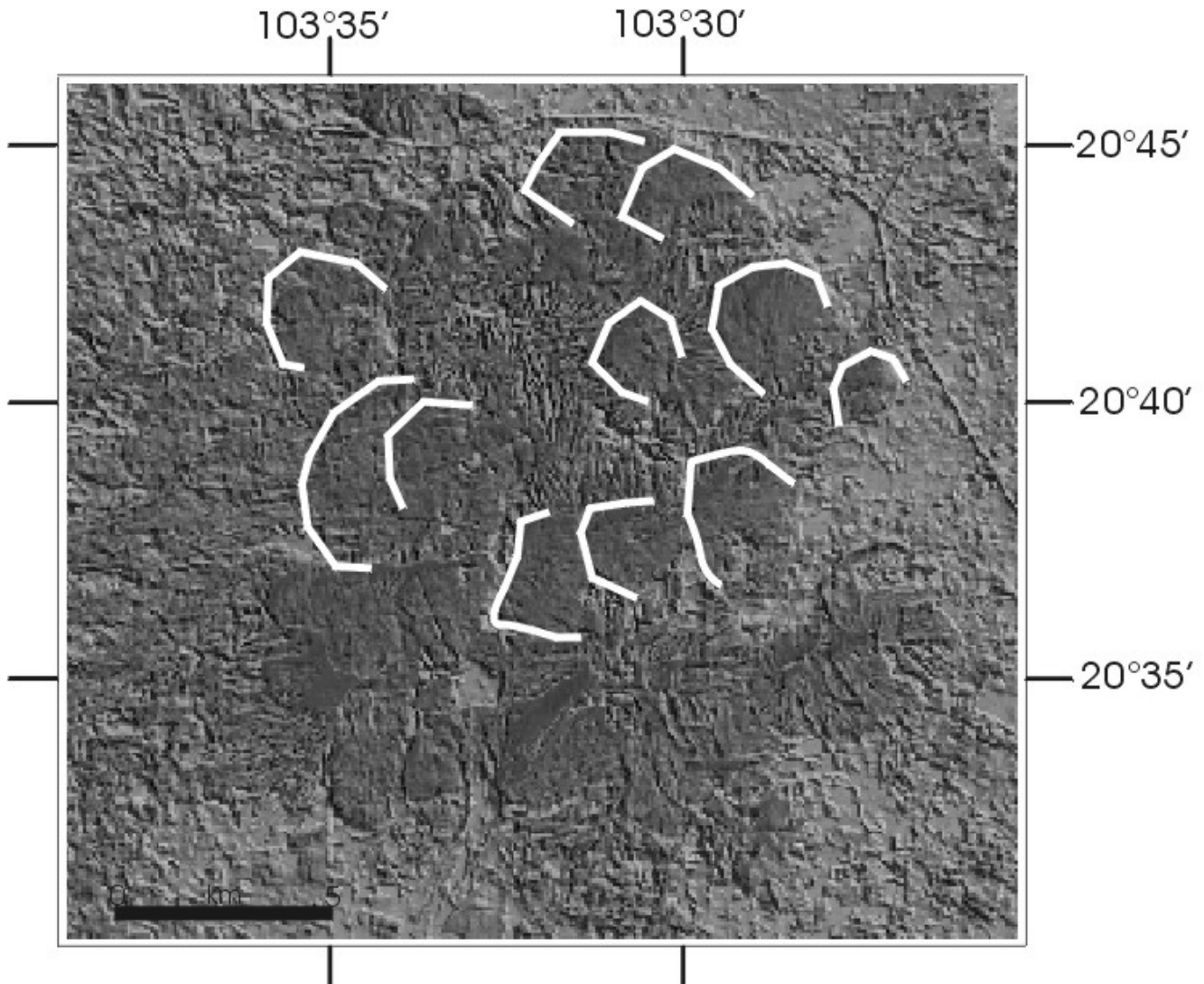
Fig. 9.- Directional filter NW-SE applied to the first principal component of La Primavera image. Lines and dots as in Fig. 8.

In Figure 8, the NE quadrant of the image is shown after a NE-SW filter was applied. The lineament corresponds to La Gotera fault. The Caldera ring fractures, the Río Caliente faults, and a portion of the Mesa El Nejahuete fault were also identified. Some lineaments are also observed among the domes Pinar de la Venta, Arroyo La Cuadrilla and Mesa La Lobera (Figure 9) which had not been reported.

The radial pattern of the drainage is clearly shown, as well as the dendritic drainage in the lower left.

DISCUSSION AND CONCLUSIONS

Band ratios, false color compositions, and principal components analysis were used to spectrally enhance the response of different minerals. They allowed the identification of areas where hydrothermal alteration is present as iron oxides and hydroxyls, as is the case of La Primavera geothermal field (Figure 10).

The identification of alteration minerals was best accomplished with the Crosta technique, as shown in Figures 5 and 6 . The presence of vegetation was interfering with the spectral response of alteration minerals, specially in the infrared bands (5 and 7); therefore the band ratios did not yield good results. False color compositions were also affected by the strong reflection of vegetation in the infrared bands (Figures 4 and 5). The minimization of the vegetation interference was obtained with the results of the principal components analysis, which identified the altered rocks. The results were checked by field observations.

The areas where hydrothermally altered rocks can be identified are constrained to the central part of the caldera,
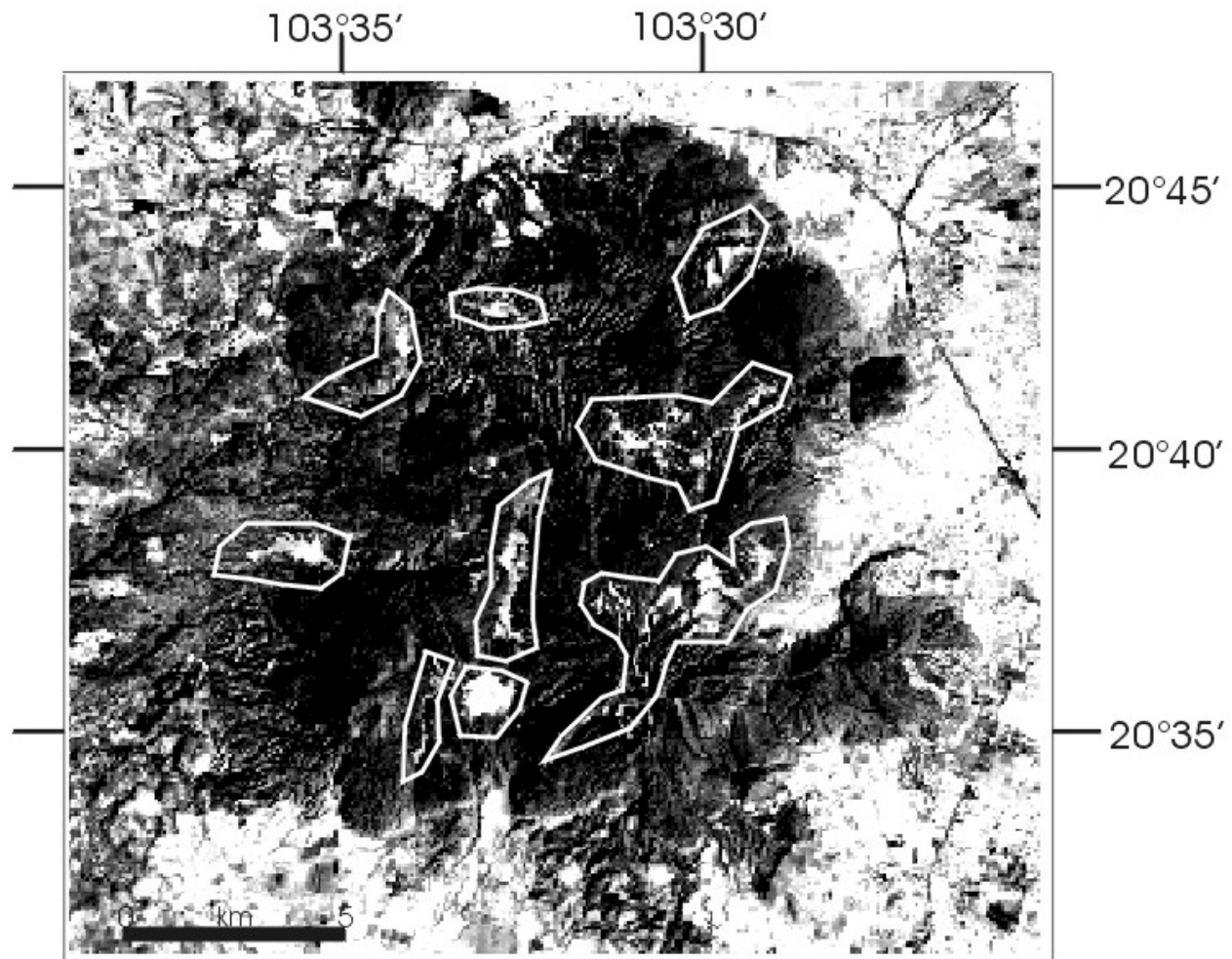
Fig. 10.- Areas where hydrothermal alteration is present as iron oxides and hydroxyls, are enclosed in polygons.

closely related with the zone where exploration wells where drilled. Intense kaolinization characterize these areas, which are shown in Figure 6. Field work in the La Primavera Geothermal Field confirmed that surface alteration was not generally present in the ring fractures that define the caldera structure. Small area with surface alteration was identified in the southern part of the field, related with the occurrence of hot springs and recent rhyolitic domes.

The main faults within the field are channels that favor the transport of the fluid. Some faults had not been defined in previous studies, as the La Gotera fault and the ring structures related to the caldera formation (shown in Figure 10). Image processing can be useful to identify hydrothermally altered rocks related with surface discharges of the geothermal system.

BIBLIOGRAPHY

ALATORRE-ZAMORA, M. A. and J. O. CAMPOS-ENRÍQUEZ, 1991. La Primavera Caldera (Mexico); structure inferred gravity and hydrogeological considerations. Geothermal and related volcanological and tectonic research in Mexico. *Geofís. Int., 31,* 4, 371-382.

CAMPOS-ENRÍQUEZ, J. O and M. A. ALATORRE-ZAMORA, 1998. Shallow Crustal Structure of the junction of the grabens of Chapala, Tepic-Zacoalco and Colima, Mexico. *Geofís. Int., 37,* 4, 263-282.

CHAVEZ, P. S. Jr. and A. YAW KWARTENG, 1989. Extracting Spectral Contrast in Landsat Thematic Mapper Image Data Using Selective Principal Component Analysis. *Photogram. Eng. Rem. Sens., 55,* 339-348.

CROSTA, A. P and J. McM. MOORE, 1989. Enhancement of Landsat Thematic Mapper Imagery for Residual Soil Mapping in SW Minas Gerais State, Brazil: A Prospecting Case History in Greenstone Belt Terrain. Proceedings of the Seventh Thematic Conference on Re-

mote Sensing for Exploration Geology, Calgary, Alberta, Canada, Oct. 2-6, pp. ERIM, 1173-1187.

DEROIN, J. P., G. R. COCHRANE, M. A. MONGILLO and P. R. L. BROWNE, 1995. Methods of remote sensing in geothermal regions: the geodynamic setting of the Taupo Volcanic Zone (North Island, New Zealand). *Int. J. Rem. Sens., 16,* 1663-1677.

DRURY, S. A. 1990. A guide to Remote Sensing: Interpreting images of the Earth. Oxford Science Publications. 199 pp.

GARDUÑO, H. and A. LÓPEZ, 1986. Fracturamiento de campos geotérmicos. *Geotermia, 2*, 277-296.

GOETZ, A. F., F. H. ROCK and B. N. ROWAN, 1983. Remote Sensing for Exploration: An Overview. *Economic Geology, 78*, 573-590.

GUTIÉRREZ-NEGRÍN, L. C. A., 1991. Recursos Geotérmicos en La Primavera, Jalisco. *Ciencia y Desarrollo, 16, 96,* 57-69.

HUNT, G. R., 1977. Spectra Signatures of Particulate Minerals in the Visible and Near Infrared. *Geophysics, 42*, 501-513.

HUNT, G. R., 1979. Near-Infrared (1.3-2.4 m) Spectra of Alteration Minerals Potential for Use in Remote Sensing. *Geophysics, 44*, 1974-1986.

HUNT, G. R. and R. P. ASHLEY, 1979. Spectra of Altered Rocks in the Visible and Near Infrared. *Economic Geology, 74*, 1613-1629.

JENSEN, J. R., 1996. Introductory digital image processing: A remote sensing perspective. 2nd ed. Prentice Hall series in Geographic information science. 318 pp.

KAUFFMANN, H. 1988. Mineral Exploration along the Aqaba-Levant Structure by use of TM-data: Concepts, processing and results. *Int. J. Rem. Sens., 9,* 1639-1658.

LILLESAND, Th. M. and R. W. KIEFER, 1987. Remote Sensing and Image Interpretation, 2nd ed.Wiley, 721 pp.

LOUGHLIN, W. P., 1991. Principal Component Analysis for Alteration Mapping. *Photogram. Eng. Rem. Sens., 57,* 1163-1169.

LUHR, J. F., S. NELSON, J. ALLAN and J. CARMICHAEL, 1985. Active rifting in South-western Mexico: Manifestations of an incipient fastward spreading- ridge jump. *Geology, 13*, 54-57.

MAHOOD, G. A., 1980a. Geological Evolution of a Pleistocene Rhyolitic Center: Sierra La Primavera, Jalisco, México. *J. Volcanol. Geotherm. Res., 8,* 199-230.

MAHOOD, G. A., 1980b. Chemical Evolution of a Pleistocene Rhyolitic Center: Sierra La Primavera, Jalisco, México. *Contrib. Mineral. Petrol., 77,* 129-149.

MAHOOD, G. A., A. H. TRUESDELL and L. A. TEMPLOS, 1983. A reconaissance geochemical study of La Primavera geothermal area, Jalisco, México. *J. Volc. Geoth. Res.,* 16 , 247-261.

MONGILLO, M. A., G. R. COCHANE, P. R. L. BROWNE and J. P. DEROIN, 1995. Application of satellite imagery to explore and monitor geothermal systems. Proceed. World Geoth. Congress., V. II, 951-956.

MOORE, G. K. and F. A. WALTZ, 1983. Objective procedure for lineaments enhancement and extraction. *Photogram. Eng. Rem. Sens., 79.* 5, 641- 647.

O'LEARY, D. W., 1979. Lineament, linear, lineation; some proposed new standards for old terms. *Geol. Soc. Am. Bull., 87,* 10, 1463-1469.

PROL-LEDESMA, R. M., 2000. Evaluation of the reconnaissance results in geothermal exploration using GIS. *Geothermics, 29,* 83-103.

RUIZ-ARMENTA, J. R. and R. M. PROL-LEDESMA, 1995. Técnicas de procesamiento de imágenes en la exploración de yacimientos minerales de origen hidrotermal. *Física de la Tierra, 7,* 105-137.

RUIZ-ARMENTA, J. R. and R. M. PROL-LEDESMA, 1998. Techniques for enhancing the spectral response of hydrothermal alteration minerals in Thematic Mapper Images of Central Mexico. *Int. J. Rem. Sens. 19,* 10, 1981-2000.

VAN DER MEER, F., P. M. VAN DIJK and A. B. WESTERHOF, 1995. Digital Classification of the contact metamorphic aureole along the Los Pedroches batholith, south-central Spain, using Landsat Thematic Mapper data. *Int. J. Rem. Sens., 16,* 1043-1062.

VENEGAS-SALGADO, S., G. RAMIREZ-SILVA, C. RO-
MERO-GONZALEZ, 1988. Campo Geotérmico de La
Primavera, Jalisco. Geología Económica de México.
Fondo de Cultura Económica, 127-141.

VILLA, S. J., M. CHACON and G. MEDINA, 1987. Utili-
zación de la relación atómica (Na/K) para identificar zo-
nas de mayor actividad hidrotermal en el campo
geotérmico de La Primavera, Jalisco. *Geotermia. Re-
vista Mexicana de Geoenergía, 3,* 3, 241-254.

WESTER, K., 1992. Spectral signature measurements and
image processing for geological remote sensing: PhD
Thesis, Department of Physical Geography, Stockholm
University, Stockholm, 130 p.

Fernández de la Vega-Márquez, T.[1], R. M. Prol-
Ledesma[2] and G. Orozco[3]

[1] *Facultad de Filosofía, UNAM, 04510 México, D.F. Mexico*
[2] *Instituto de Geofísica, UNAM, 04510 México, D.F. Mexico*
[3] *Schlumberger, Melbourne, Australia*